

# Black hole mass estimation from X-ray variability measurements in AGN

M. Nikolajuk<sup>1</sup>, I.E. Papadakis<sup>2</sup> and B. Czerny<sup>1</sup>

<sup>1</sup> *N. Copernicus Astronomical Centre, Bartycka 18, 00-716 Warsaw, Poland*

<sup>2</sup> *Physics Department, University of Crete, 71 003, Heraklion, Crete, Greece*

11 November 2018

## ABSTRACT

We propose a new method of estimation of the black hole masses in AGN based on the normalized excess variance,  $\sigma_{\text{nxss}}^2$ . We derive a relation between  $\sigma_{\text{nxss}}^2$ , the length of the observation,  $T$ , the light curve bin size,  $\Delta t$ , and the black hole mass, assuming that (i) the power spectrum above the high frequency break,  $\nu_{\text{bf}}$ , has a slope of  $-2$ , (ii) the high frequency break scales with black hole mass, (iii) the power spectrum amplitude (in *frequency*  $\times$  *power* space) is universal and (iv)  $\sigma_{\text{nxss}}^2$  is calculated from observations of length  $T < 1/\nu_{\text{bf}}$ . Values of black hole masses in AGN obtained with this method are consistent with estimates based on other techniques such as reverberation mapping or the  $M_{\text{BH}}$ -stellar velocity dispersion relation. The method is formally equivalent to methods based on power spectrum scaling with mass but the use of  $\sigma_{\text{nxss}}^2$  has the big advantage of being applicable to relatively low quality data.

**Key words:** galaxies: active – galaxies: Seyfert – X-rays: galaxies

## 1 INTRODUCTION

The X-ray emission of active galactic nuclei (AGN) displays variations over a wide range of time scales. The first convincing demonstration of this phenomenon came with the *EXOSAT* ‘long looks’ (Lawrence et al. 1987; McHardy & Czerny 1987). The data showed no characteristic time-scales, and the power spectral density function (PSD) showed a ‘red-noise’ shape. At the same time, it was also noticed that more luminous sources show slower variations. Various methods have been used in the past in order to determine the X-ray variability amplitude of AGN: determination of the ‘two-folding’ time-scale (i.e. the time-scale for the emitted flux to change by a factor of two), calculation of the PSD amplitude at a given frequency, and estimation of the so called ‘normalized excess variance’ ( $\sigma_{\text{nxss}}^2$ , i.e. the variance of a light curve normalized by its mean squared after correcting for the experimental noise). In all cases, these quantities appear to anti-correlate with the source luminosity (Barr & Mushotzky 1986; Lawrence & Papadakis 1993; Green, McHardy & Lehto 1993; Nandra et al. 1997; Turner et al. 1999; Leighly 1999; Markowitz & Edelson 2001). One possible explanation for the observed anti-correlation between the X-ray variability amplitude and X-ray luminosity,  $L_X$ , is that more luminous AGN have larger black hole masses ( $M_{\text{BH}}$ ) as well. In this case, as  $M_{\text{BH}}$  increases, so does the size of the X-ray source, and a change of the source luminosity by a constant fraction takes relatively longer; equivalently, variability amplitude measured at a fixed timescale should decrease with mass. The significant progress in the

measurement of the black hole (BH) mass in the centers of nearby galaxies has made it possible to actually directly test the dependence of the X-ray variability amplitude on  $M_{\text{BH}}$  in AGN. The data show that  $\sigma_{\text{nxss}}^2$  measured at a certain timescale is indeed anti-correlated with  $M_{\text{BH}}$  (Lu & Yu 2001; Bian & Zao 2003; Papadakis 2004).

If there is an intrinsic correlation between X-ray variability and  $M_{\text{BH}}$ , then X-ray variability measurements could be used in order to measure the central black hole mass in these objects. This possibility has already been studied in the past. Hayashida et al. (1998) and Czerny et al. (2001) have used the PSD normalized by the square of the mean flux as a measure of the X-ray variability of a source. By calculating the ratio of the frequencies at which the PSD  $\times$  *frequency* has a certain value in AGN and Cyg X-1, they were able to estimate the  $M_{\text{BH}}$  in AGN. Recently, long, well-sampled *RXTE* light curves have been used in order to accurately estimate the X-ray PSD of AGN. One of the main results from these studies has been the unambiguous detection of a characteristic ‘break frequency’,  $\nu_{\text{bf}}$ , at which the power spectrum changes its slope from a value of  $-2$  to  $-1$  above and below  $\nu_{\text{bf}}$ , respectively (Uttley et al. 2002; Markowitz et al. 2003). This break frequency is analogous to the high frequency break in galactic sources and should not be confused with the low frequency break, where the spectrum changes slope from  $-1$  above to  $0$  below. This high frequency break appears to correlate well with  $M_{\text{BH}}$ , in the sense that  $1/\nu_{\text{bf}} \propto M_{\text{BH}}$  (Markowitz et al. 2003). Thus another way to estimate  $M_{\text{BH}}$  is through the determination

of  $\nu_{\text{bf}}$  in the X-ray PSD of a source. However, this method requires rather long, high quality data.

We propose a new method to estimate  $M_{\text{BH}}$  in AGN, which may be used even for relatively low quality and/or short data coverage. The method is based on the use of  $\sigma_{\text{nxss}}^2$  as a measure of their X-ray variability amplitude, and takes Cyg X-1 as a reference point. Using recent, archival *RXTE* and *ASCA* light curves of 21 AGN, we estimate their  $M_{\text{BH}}$ , and we compare our results with  $M_{\text{BH}}$  estimates which are based on other methods. We find that the accuracy of the  $M_{\text{BH}}$  estimates using our new method is roughly similar to the accuracy of the estimates with well established methods like reverberation mapping. Furthermore, the  $\sigma_{\text{nxss}}^2$  estimation of an X-ray light curve is rather easy and straightforward. Consequently, as long as typical AGN observations performed by present day satellites (like *XMM-Newton* and *CHANDRA*) detect significant variations, they can be used to estimate  $\sigma_{\text{nxss}}^2$  and hence  $M_{\text{BH}}$ , using the method which we present in this work. It is possible then that the use of our method can provide  $M_{\text{BH}}$  estimates for a large number of AGN in the near future.

## 2 THE RELATION BETWEEN BH MASS AND EXCESS VARIANCE

The scaling of the PSD with mass is most conveniently discussed after multiplying the normalized PSD by the frequency  $\nu$ . We assume here that the break frequency,  $\nu_{\text{bf}}$ , scales with the mass:  $\nu_{\text{bf}} \propto M_{\text{BH}}^{-1}$ , but the amplitude of the normalized PSD  $\times \nu$  part at the frequency break does not depend on mass. We specifically define this normalization at  $\nu_{\text{bf}}$  and call it the PSD amplitude,

$$PSD_{\text{amp}} = P(\nu_{\text{bf}}) \times \nu_{\text{bf}}, \quad (1)$$

where  $P(\nu)$  is the power spectrum normalized to the mean squared. Recently, Papadakis (2004) has showed that this quantity is indeed similar in a few well studied Seyfert 1 galaxies.

Let us suppose that an AGN is observed for a period  $T < 1/\nu_{\text{bf}}$ , and that the resulting light curve is binned using a bin size of  $\Delta t$ . The excess variance of the light curve is equal to the integral of the PSD,

$$\sigma_{\text{nxss}}^2 = \int_{1/T}^{1/2\Delta t} P(\nu) d\nu \quad (2)$$

Let us also suppose that  $P(\nu) = A(\nu/\nu_{\text{bf}})^{-2}$ , where  $A = PSD_{\text{amp}}/\nu_{\text{bf}}$  and  $PSD_{\text{amp}}$  is constant, and that  $\nu_{\text{bf}} = B/M_{\text{BH}}$ , where  $B$  is another constant. Under these assumptions,

$$\sigma_{\text{nxss}}^2 = PSD_{\text{amp}} \frac{B}{M_{\text{BH}}} (T - 2\Delta t). \quad (3)$$

The equation above can be re-written as follows,

$$M_{\text{BH}} = C(T - 2\Delta t)/\sigma_{\text{nxss}}^2, \quad (4)$$

where  $C = PSD_{\text{amp}}B$ . Eq. (4) can be used to estimate  $M_{\text{BH}}$  provided the  $\sigma_{\text{nxss}}^2$  of a source has been estimated, and  $C$  is known. In order to determine  $C$ , we used the results from the PSD analysis of a Galactic black hole candidate, namely Cyg X-1.

The X-ray PSD of this source has been extensively studied the last twenty years or so (Kemp et al. 1978; Gierliński et al. 1999; Nowak et al. 1999; Churazov et al. 2001; Pottschmidt et al. 2003). In its low/hard state, the PSD of the source can be roughly represented as a power law with a high frequency slope of  $-2$ , which breaks to a slope of  $-1$  below  $2 - 3$  Hz, and then to a slope of zero below  $\sim 0.2 - 0.02$  Hz (Nowak et al. 1999; Pottschmidt 2003). Assuming that Eq. (4) holds for Cyg X-1 as well, and adopting the value of  $10 M_{\odot}$  for its black hole mass (Nowak et al. 1999; Gierliński et al. 1999 and references therein), we determined the value of  $C$  as follows.

We used the results from the PSD analysis of 130 *RXTE* observations of Cyg X-1 reported by Pottschmidt et al. 2003. They calculated the PSD for each observation and fitted them using Lorentzian functions. The *RXTE* observations cover a long period of time (from December 1997 to July 2001) in which Cyg X-1 was mainly in its hard state. We chose 68 observations, carefully avoiding data from soft or failed transition states. We calculated the excess variance using the relation  $\sigma_{\text{nxss}}^2 = \int_{10\text{Hz}}^{+\infty} P(\nu) d\nu$ , where the lower frequency limit was chosen in such a way that it will always be higher than  $\nu_{\text{bf}}$  in this source. Using Eq. (4), with  $M_{\text{BH}} = 10 M_{\odot}$ ,  $\Delta t = 0$ , and  $T = 1/(10 \text{ Hz}) = 0.1$  sec, we find that  $C$  varies between  $\sim 0.7$  and  $\sim 1.3$ , with the arithmetic mean being  $C = 0.96 \pm 0.02$ . We accept this value for the normalization constant  $C$  in Eq. (4).

## 3 NEW $M_{\text{BH}}$ ESTIMATES FOR 21 AGN

In order to investigate the accuracy of our method, we selected for analysis several AGN with known black hole masses and recently obtained *RXTE* or *ASCA* light curves. First, we estimated the  $\sigma_{\text{nxss}}^2$  of each light curve using the relation (Nandra et al., 1997),

$$\sigma_{\text{nxss}}^2 = \frac{1}{N_{\text{data}}} \frac{1}{\bar{x}^2} \sum_{i=1}^{N_{\text{data}}} [(x_i - \bar{x})^2 - \sigma_i^2], \quad (5)$$

where  $N_{\text{data}}$  is the number of data points, and  $\bar{x}, \sigma_i$  are the unweighted, arithmetic mean and error of the  $x_i$ , respectively. Then, using Eq. (4) we estimated  $M_{\text{BH}}$ , and compared our  $M_{\text{BH}}$  estimates with the existing values from literature based on the reverberation mapping technique or the measurement of stellar velocity dispersion (Section 3.2, Table 1).

### 3.1 Remarks about preparation of the data

*RXTE* has regularly observed a large number of AGN over the last few years, providing long light curves with good signal to noise (S/N). For almost all the objects listed in Table 1 we have retrieved 2 – 9 keV PCA background subtracted light curves from the standard data products ('Std-Props') archive of *RXTE* (detailed information about the data in this archive is given at the *RXTE* mission web site). There are no archival *RXTE* data for 3 AGN with previously estimated  $M_{\text{BH}}$  (namely PG1211+143, NGC4395 and NGC4593). For these sources we retrieved 2 – 10 keV, *ASCA* light curves from the TARTARUS database. We used background subtracted GIS and SIS light curves which we combined in all cases, except from the first observation of

**Table 1.** Previous and new  $M_{\text{BH}}$  estimates for 21 AGN

Name	$M_{\text{BH,L}}$ ( $\times 10^7 M_{\odot}$ )	$M_{\text{BH},\sigma_{\text{nxss}}^2}$ ( $\times 10^7 M_{\odot}$ )	Proposal number
3C120	6.3 (1,2)	14.5	R/P30404(3)
3C390.3	35.5 (1)	26.8	R/P10340(7)
Akn120	18.6 (1)	5.6	R/P30232(1)
IC4329A	0.6 (1)	12.3	R/P40153(2) R/P20315(2) R/P10313(4) R/P50706(1)
IC5063 (S2)	5.5 (2)	(0.19) 3.8	R/P10337(1)
Mrk348 (S2)	1.6 (2)	7.5	R/P10326(3)
Mrk509	7.5 (1)	7.0	R/P10311(8)
Mrk766 (★)	0.35 (2)	(0.0066) 0.132	R/P60135(23)
NGC3227	4.1 (1,3)	2.2	R/P40151(6) R/P10292(3)
NGC3516	1.7 (3)	1.7	R/P50159(1) R/P20316(4) R/P30224(2)
NGC3783	1.0 (1)	0.83	R/P10297(2,1) R/P30227(1)
NGC4051 (★)	0.05 (5)	(0.0014) 0.028	R/P50153(128)
NGC4151	1.4 (1)	1.9	R/P50155(2) R/P00022(3) R/P00024(4)
NGC4395	0.007(6)	0.022	A/76006000(2)
NGC4593	0.66 (3)	0.60	A/71024000(3) A/75023010(1)
NGC5506 (★)	8.8 (4)	(0.32) 6.4	R/P20318(10)
NGC5548	9.2 (1,7)	12.3	R/P30220(2) R/P10297(3) R/P30218(3)
NGC7469	0.7 (1)	1.3	R/P10315(20)
PG0052+251	26.1(1)	10.0	R/P40157(1) R/P20338(1)
PG0804+761	7.6 (1)	5.6	R/P40157(3)
PG1211+143 (★)	3.2 (1)	(0.40) 8.1	A/70025000(1)

Col. (1) lists the object name and type: (S2) denote Seyfert 2 objects, (★) - Narrow Line Seyfert 1. All other objects are classified as Seyfert 1 or quasars. Col. (2) lists the  $M_{\text{BH,L}}$  values taken from literature. The numbers in parentheses in Col. (2) correspond to the following references: (1) Kaspi et al. (2000), (2) Woo & Urry (2002), (3) Onken et al. (2003), (4) Papadakis (2004), (5) Shemmer et al. (2003), (6) Filippenko & Ho (2003), (7) Peterson & Wandel (2000). Col. (3) lists the  $M_{\text{BH},\sigma_{\text{nxss}}^2}$  values obtained in this work. For NLS1s, the values in parentheses are the  $M_{\text{BH}}$  values found using Eq. (3), while the values listed below are multiplied by a factor of 20 (see text for details). Col. (4) lists the observation details. The first letter refers to the satellite (R – RXTE, A – ASCA), the number that follows refers to proposal number, and we list the number of light curve parts,  $N_{\text{p}}$ , which we used in order to determine  $\sigma_{\text{nxss}}^2$ , in parentheses.

NGC4593. In this case we used the GIS data only, as there were many missing points in the SIS light curve.

The character of the obtained light curves depended mostly on the type of the monitoring. A number of the light curves came from sparse extensive monitoring. The source was observed typically for 10 ksec once per day, for several

days. For example, 3C390.3 was observed usually once per day, for 2 months, with a single observation lasting about 3 ksec. Such light curves were binned to 5400 sec (roughly the orbital period of the satellite). If the resulting light curve consisted predominantly of single points separated by a day, then the remaining few consecutive data points were averaged to create a uniformly covered light curve.

Other light curves came from intensive monitoring. The source was observed continuously for 40 ksec or more, with gaps only caused by earth occultation. For example, NGC3516 was observed for over one day. The observational campaign was sometimes repeated or supplemented by sparse extensive monitoring. NGC7469 was almost continuously observed for about 1 month: 10 to 20 ksec exposures were made almost every day. Such light curves were also binned to 5400 s.

Several sources were occasionally observed for 10 – 40 ksec. The bin size used for these light curves typically varied from 512 s to 5400 s, depending on the length of the data and the S/N ratio.

The light curve of PG0052+251 was binned to 10800 s in order to increase the S/N ratio. The light curve from continuous monitoring of NGC4593 was binned to 2048 s and divided into separate sets of 30 ksec duration in order to estimate  $\sigma_{\text{nxss}}^2$  in more than 2 sub-parts. Even shorter bin size was requested for NLS1 sources, as discussed below.

The long light curves were divided into separate shorter strings of length  $T$ , as required by the condition  $T < 1/\nu_{\text{bf}}$  (see Section 2). The value of  $\nu_{\text{bf}}$  for each source was estimated from the previous  $M_{\text{BH}}$  estimates, using the  $1/\nu_{\text{bf}}-M_{\text{BH}}$  relation of Markowitz et al. (2003). The PSD break frequencies of 3 NLS1 objects (NGC4051, NGC4253/Mrk766, and NGC5506) are high (see McHardy et al. 2003; Vaughan & Fabian 2003 and Uttley et al. 2002). Consequently, their light curves were divided into parts with  $T = 1.25, 2,$  and  $10$  ksec, respectively. In order to have as many points as possible in them, we used a bin size of 16 s for the NGC4051 and Mrk766 light curves, and a bin size of 128 s in the case of NGC5506. In some cases, even if  $T < 1/\nu_{\text{bf}}$ , long, well sampled light curves were also divided into shorter parts in order to increase the number of  $\sigma_{\text{nxss}}^2$  estimates.

The  $\sigma_{\text{nxss}}^2$  values were calculated for each short light curve or each substring of a long light curve separately. The number of light curve sub-parts ( $N_{\text{p}}$ ) used for the  $M_{\text{BH}}$  estimation of each source is listed in column (4) of Table 1. In the case when  $N_{\text{p}} > 1$ , we used the average  $\sigma_{\text{nxss}}^2$  value to derive the black hole mass from Eq. (4).

## 3.2 Results

The values of the black hole masses obtained from Eq. (4) are given in Table 1.

Column (1) in this table lists the names of AGN. Four objects are classified as ‘Narrow Line Seyfert 1’ (NLS1), while the others are classical broad line Seyfert 1 (S1)/quasars (QSO), and Seyfert 2 (S2) objects. Column (2) gives the  $M_{\text{BH}}$  estimates taken mostly from Kaspi et al. (2000), and they correspond to the mean value of their ‘mean’ and ‘rms’ values. In cases where we found more than one  $M_{\text{BH}}$  estimate for an object, the value listed in Table 1 corresponds to the mean of the respective estimates. Column (3) gives our mass determination based on X-ray variability.

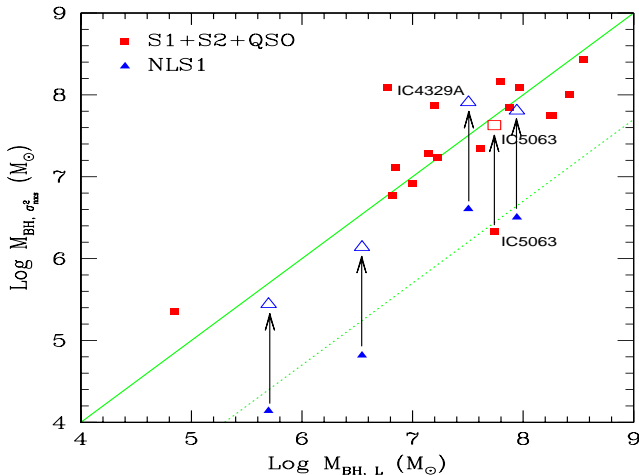


**Figure 1.** Black hole mass estimates using the method presented in this work ( $M_{\text{BH}, \sigma_{\text{NXS}}^2}$ ) plotted versus the literature estimates ( $M_{\text{BH}, \text{L}}$ ), for the objects listed in Table 1. Solid squares and solid triangles show the classical Seyfert 1/Seyfert 2/quasars and the NLS1 estimates, respectively. Open triangles and the open square show the NLS1 and IC5063 estimates after they have been multiplied by a factor of 20 (see text for details). The solid line shows the  $M_{\text{BH}, \sigma_{\text{NXS}}^2} = M_{\text{BH}, \text{L}}$  relation.

Fig. 1 shows a comparison of the two mass determinations. Generally, the agreement between  $M_{\text{BH}, \sigma_{\text{NXS}}^2}$  and  $M_{\text{BH}, \text{L}}$  is quite good for the classical Seyferts (filled squares), but not in the case of NLS1s (filled triangles). Our  $M_{\text{BH}}$  estimates for the latter are significantly smaller than  $M_{\text{BH}, \text{L}}$ . Excluding NLS1s, we find that on average,  $\langle M_{\text{BH}, \sigma_{\text{NXS}}^2} / M_{\text{BH}, \text{L}} \rangle = 2.44 \pm 1.16$ . Two other sources with the largest differences between  $M_{\text{BH}, \sigma_{\text{NXS}}^2}$  and  $M_{\text{BH}, \text{L}}$  are IC5063 and IC4329A; excluding also those sources from our sample we find that on average,  $\langle M_{\text{BH}, \sigma_{\text{NXS}}^2} / M_{\text{BH}, \text{L}} \rangle = 1.41 \pm 0.31$ .

The results for NLS1 galaxies can be reconciled with the previous mass determination if we multiply our  $M_{\text{BH}}$  NLS1 estimates by a factor of 20 (open triangles in Fig. 1). Interestingly, when we multiply our IC5063 estimate by the same factor 20 as for other NLS1, the new value becomes very similar to  $M_{\text{BH}, \text{L}}$  for that object. This source is classified as S2 with broad polarized Balmer lines (Véron-Cetty & Véron, 2001). Colina et al. (1991) found strong evidence for the presence of a hidden, luminous source in the nucleus of IC5063. Perhaps then, this S2 galaxy may host a NLS1 rather than a S1 nucleus, like NGC5506 (Nagar et al. 2002). In this light we suggest that IC5063 is a hidden NLS1.

The source of the problems with IC4329A is more difficult to understand. If we use the stellar velocity dispersion measurement of  $225 \text{ km s}^{-1}$  (Oliva et al., 1999) for this object, together with the  $M_{\text{BH}}$ -stellar velocity dispersion relation of Tremaine et al. (2002), we obtain  $M_{\text{BH}} \sim 2.2 \times 10^8 M_{\odot}$ , entirely consistent with our estimate for this source. Marziani et al. (1992) found that this source has large extinction and they gave  $E(B-V) \simeq 0.8$ . After correcting the optical luminosity,  $\nu L_{\nu}$ , at  $5100 \text{ \AA}$  for the large extinction, Nikolajuk (2004) finds  $M_{\text{BH}} = 3.9 \times 10^8 M_{\odot}$ , using the accretion disk method. This value is again consistent with the

$M_{\text{BH}}$  estimate listed in Table 1. Therefore, the value given by Kaspi et al. (2000) may be too small.

When we exclude IC4329A from our sample but we consider S1 mass estimates, together with the scaled NLS1 and IC5063 estimates, then  $\langle M_{\text{BH}, \sigma_{\text{NXS}}^2} / M_{\text{BH}, \text{L}} \rangle = 1.30 \pm 0.25$ . This result suggests that the new method we propose for the  $M_{\text{BH}}$  estimation in AGN provides estimates which are consistent with the estimates based on the reverberation mapping technique or the  $M_{\text{BH}}$ -stellar velocity dispersion relation.

## 4 DISCUSSION

In this work we propose a new method for the estimation of black hole mass in AGN. The method is based on the use of the ‘normalized excess variance’,  $\sigma_{\text{NXS}}^2$ , as estimated from X-ray light (Eq. 5). We find a simple expression between  $\sigma_{\text{NXS}}^2$  and  $M_{\text{BH}}$  (Eq. 4), if we assume that the power spectrum in AGN has a ‘universal’ form: (1) there is a break frequency which scales with  $M_{\text{BH}}$ , (2) the PSD slope above the break frequency is  $-2$ , and (3) the PSD amplitude below the break frequency is roughly constant in all objects, independent of  $M_{\text{BH}}$  (see Section 2). Note that the method is applicable to 2–10 keV light curves, as the PSD may be different in other energy bands (e.g. Nandra & Papadakis 2001; Vaughan & Fabian 2003; Vaughan et al. 2003).

Using our method on archival *RXTE*, and *ASCA*, 2–10 keV light curves, we estimated  $M_{\text{BH}}$  in 21 AGN, with previously known  $M_{\text{BH}}$  estimates. The comparison between the new and past  $M_{\text{BH}}$  estimates indicates that the method works very well for ‘classical’ AGN, i.e. S1, S2 galaxies and quasars. The  $M_{\text{BH}}$  values that we find with the proposed X-ray variability method are comparable to the values determined with other methods. However, there seems to be a significant disagreement for NLS1 objects. Their mass estimates, determined from the X-ray variability method, are significantly smaller than the  $M_{\text{BH}}$  estimates which are based on other methods. The basic issue, that there is a shift in the X-ray variability amplitude of NLS1 and ‘classical’ AGN of the same mass, was already noticed by Czerny et al. (2001). Furthermore, Papadakis (2004) and McHardy et al. (2003) have showed that the break frequency  $\nu_{\text{bf}}$  of NLS1 is probably higher than the respective frequency in the power spectra of ‘classical’ AGN with the same black hole mass. If  $B^{\text{NLS1}} \sim 20 \times B^{\text{class}}$  (Papadakis 2004), where  $B$  is the constant defined in Section (2), and  $PSD_{\text{amp}}$  is the same for both classes of objects, then since  $C = PSD_{\text{amp}} B$ , we should expect that  $C^{\text{NLS1}} \sim 20 \times C^{\text{class}}$ . If we adopt this view, then we obtain an excellent agreement between the  $M_{\text{BH}}$  estimates which are based on the present X-ray variability method and the previous estimates for all objects, both ‘classical’ AGN and NLS1s.

The method we present here is based on the assumption of a ‘universal’ power spectrum shape in AGN. Consequently, it is formally equivalent to other methods which directly use the scaling of a certain power spectrum characteristic (like the break frequency, or a fixed PSD value) with  $M_{\text{BH}}$  (e.g. Hayashida et al. 1998; Czerny et al. 2001; Markowitz et al. 2003). However, as our method requires the estimation of  $\sigma_{\text{NXS}}^2$  only, it should be applicable for many more cases than methods which require the estimation of the PSD, as the latter is much more complicated.

Present day satellites like *XMM-Newton* and *CHANDRA* will soon provide a large number of AGN light curves with a typical exposure time of 30 – 50 ksec. Due to the low internal background of their detectors, most of these light curves should be of high signal to noise in the 2 – 10 keV band. Furthermore, because of their long orbital periods, light curves (as long as  $\sim 1.5$  days) will be evenly sampled. Provided that significant variations are observed, they could be used to estimate  $\sigma_{\text{nxss}}^2$ , and hence  $M_{\text{BH}}$  through Eq. (4).

The choice of the bin size,  $\Delta t$ , is not crucial and should depend mainly on the average count rate. It needs to be large enough in order to minimize the effects of the experimental Poisson noise, but at the same time the resulting number of the points in the light curve,  $N_{\text{data}}$ , should also be large (at least larger than 10).

The choice of the length of a single data string,  $T$ , must satisfy the requirement  $1/T > \nu_{\text{bf}}$ . If  $\nu_{\text{bf}}$  for a given object is not known in advance, this condition should be checked *a posteriori*. For NLS1, the length should be  $\sim 20$  times smaller than the appropriate  $T$  value for classical AGN, according to the results of the present work.

Apart from observational errors, the determination of the  $\sigma_{\text{nxss}}^2$  is biased by intrinsic statistical error connected with the specific shape of the power spectrum (Vaughan et al. 2003). Averaging over several independent variance measurements performed at various epochs reduces the error. If we have a single long light curve the error reduction is less efficient but can be assessed through simulations. We performed such simulations for NGC 5506 light curve (6 times longer than  $1/\nu_{\text{bf}}$ ) with many gaps, and with typical duration of a single string of  $10^4$  s. Systematic ‘leak’ of the power from long to shorter timescales appeared to be negligible, and the intrinsic statistical scatter was  $\Delta \log \sigma_{\text{nxss}}^2 = {}^{+0.20}_{-0.19}$ , at 90 per cent confidence level.

Finally, we determined the constant  $C$  in Eq. (4) assuming that  $M_{\text{BH}} = 10 M_{\odot}$  for Cyg X-1. However, if a higher value of  $\sim 20 M_{\odot}$  is more appropriate for this object (e.g. Ziółkowski 2004), then  $C$  and the  $M_{\text{BH}}$  estimates listed in Table 1 should be increased by a factor of  $\sim 2$ . Such a change would, however, actually introduce a discrepancy between the masses estimated from the present X-ray variability and from other methods. Although the mass determination by the reverberation method may also contain a systematical error of the order of a factor 2 – 3 (see Krolik 2001), this possibility underlines the importance of the accurate determination of the properties of Cyg X-1 as this object is routinely used as a reference source.

## 5 CONCLUSIONS

- We propose a new method based on measurements of  $\sigma_{\text{nxss}}^2$  of X-ray variability of AGN to  $M_{\text{BH}}$  estimates. The estimates of black hole masses in AGN obtained from our method ( $M_{\text{BH}, \sigma_{\text{nxss}}^2}$ ) are consistent with the estimates based on other techniques such as the reverberation mapping technique or the  $M_{\text{BH}}$ -stellar velocity dispersion relation.

- The constant  $C$  in Eq. (4) is equal to 0.96 for ‘classical’ AGN and 19.2 (i.e. 20 times larger) for NLS1

- We suggest that IC5063, classified as S2 galaxy, is in fact a hidden NLS1.

## ACKNOWLEDGMENTS

This work was partially supported by grants 2P03D 00322 and PBZ-KBN-054/P03/2001. This research has made use of the TARTARUS database, which is supported by Jane Turner and Kirpal Nandra under NASA grants NAG5-7385 and NAG5-7067. IEP thanks CAMK for their hospitality.

## REFERENCES

- Barr P., Mushotzky R.F., 1986, *Nat*, 320, 421  
 Bian W., Zao Y., 2003, *MNRAS*, 343, 164  
 Churazov E., Gilfanov M., Revnivtsev M., 2001, *MNRAS*, 321, 759  
 Colina L, Sparks W.B., Macchetto F., 1991, *ApJ*, 370, 102  
 Czerny B., Nikolajuk M., Piasecki M., Kuraszekiewicz J., 2001, *MNRAS*, 325, 865  
 Filippenko A.V., Ho L.C., 2003, *ApJ*, 588, L13  
 Gierliński M., Zdziarski A.A., Poutanen J., Coppi P.S., Ebisawa K., Johnson W.N., 1999, *MNRAS*, 309, 496  
 Green A.R., McHardy I.M., Lehto H.J., 1993, *MNRAS*, 265, 664  
 Hayashida K., Miyamoto S., Kitamoto S., Negoro H., Inoue H., 1998, *ApJ*, 500, 642  
 Kaspi S., Smith P.S., Netzer H., Maoz D., Buell T.J., Giveon U., 2000, *ApJ*, 533, 631  
 Kemp J.C., Herman L.C., Barbour M.S., 1978, *AJ*, 83, 962  
 Krolik J.H., 2001, *ApJ*, 551, 72  
 Lawrence A., Papadakis I.E., 1993, *ApJ*, 414, L85  
 Lawrence A., Watson M.G., Pounds K.A., Elvis M., 1987, *Nat*, 325, 694  
 Leighly K.M., 1999, *ApJS*, 125, 297  
 Lu Y., Yu Q., 2001, *MNRAS*, 324, 653  
 Markowitz, A., Edelson, R., 2001, *ApJ*, 547, 684  
 Markowitz, A. et al., 2003, *ApJ*, 593, 96  
 Marziani P., Calvani M., Sulentic J.W., 1992, *ApJ*, 393, 658  
 McHardy I., Czerny B., 1987, *Nat*, 325, 696  
 McHardy I., Papadakis I.E., Uttley P., Page M., Mason K., 2003, *MNRAS*, submitted (astro-ph/0311220)  
 Nagar N.M., Oliva E., Marconi A., Maiolino R., 2002, *A&A*, 391, L21  
 Nandra K., George I.M., Mushotzky R.F., Turner T.J., Yaqoob T., 1997, *ApJ*, 476, 70  
 Nandra K., Papadakis, I. E., 2001, *ApJ*, 554, 710  
 Nikolajuk M., 2004, *A&A*, in preparation  
 Nowak M.A., Vaughan B.A., Wilms J., Dove J.B., Begelman M.C., 1999, *ApJ*, 510, 874  
 Oliva E., Origlia L., Maiolino R., Moorwood A.F.M., 1999, *A&A*, 350, 90  
 Onken C.A., Peterson B.M., Dietrich M., Robinson A., Salamanca I.M., 2003, *ApJ*, 585, 120  
 Papadakis I.E., 2004, *MNRAS*, 348, 207  
 Peterson B.M., Wandel A., 2000, *ApJ*, 540, L13  
 Pottschmidt K. et al., 2003, *A&A*, 407, 1039  
 Shemmer O., Uttley P., Netzer H., McHardy I.M., 2003, *MNRAS*, 343, 1341  
 Tremaine S., et al. 2002, *ApJ*, 574, 740  
 Turner T.J., George I.M., Nandra K., Turcan D., 1999, *ApJ*, 524, 667  
 Uttley P., McHardy I., Papadakis I.E., 2002, *MNRAS*, 332, 231  
 Vaughan S., Edelson R., Warwick R.S., Uttley P., 2003, *MNRAS*, 345, 1271  
 Vaughan S., Fabian A.C., 2003, *MNRAS*, 341, 496  
 Vaughan S., Fabian A.C., Nandra K., 2003, *MNRAS*, 339, 1237  
 Véron-Cetty M.-P., Véron P., 2001, *A&A*, 374, 92  
 Woo J.H., Urry M.C., 2002, *ApJ*, 579, 530  
 Ziółkowski, 2004, *MNRAS*, submitted